GEOPHYSICAL RESEARCH LETTERS, VOL. 29, NO. 5, 1075, 10.1029/2001GL014097, 2002

Offshore Ekman transport and Ekman pumping off Peru during the 1997–1998 El Niño

David Halpern

Jet Propulsion Laboratory, California Institute of Technology, Pasadena, CA 91109, USA

Received 14 September 2001; accepted 11 December 2001; published 14 March 2002.

[1] Satellite ocean vector wind measurements are used to describe onshore-offshore Ekman transport and Ekman pumping/suction (i.e., downward/upward velocity) in the coastal ocean at 15°S off Peru, where upwelling is the dominant physical process. Normal and El Niño conditions are defined for May 1992 – April 1997 and May 1997 – May 1998, respectively. During normal conditions, both Ekman suction and offshore Ekman transport produced upwelling. During the El Niño, the May–August speed of Ekman pumping (-9×10^{-6} m s^{-1}) was nearly 4 times larger than the normal speed of Ekman suction and offshore Ekman transport nearly doubled. The strong Ekman pumping may be the source for the deepened coastal thermocline during El Niño, although the evidence is not conclusive because of the absence of in situ observations. *INDEX TERMS:* 4279 Oceanography: General: Upwelling and convergences; 4522 Oceanography: Physical: El Niño; 4516 Oceanography: General: Eastern boundary currents; 4223 Oceanography: Physical: Descriptive and regional oceanography

1. Introduction

[2] Upwelling occurs along a coastline when surface wind stress produces offshore Ekman transport or when wind stress curl produces upward motion at the bottom of the Ekman layer. Ekman transport is proportional to the wind stress and inversely proportional to the sine of the latitude [*Sverdrup et al.*, 1942, p. 498] and, along a coastline, can be represented by $\tau_{alongshore}/(\rho f)$, where $\tau_{alongshore}$ is the alongshore component of surface wind stress, ρ is seawater density (1025 kg m^{-3}), and f is the Coriolis parameter ($=2\Omega\sin\theta$, with Ω and θ equal to Earth's angular velocity and latitude, respectively). Equatorward wind stress along a western coastline produces offshore Ekman transport. Wind stress curl vertical velocity at the bottom of the Ekman layer, W_{EK}, named Ekman suction if upward and Ekman pumping if downward, is [*Stommel*, 1958]

$$W_{EK} = (\text{curl}\ \tau)/(\rho f) + (\beta\tau_x)/(\rho f^2)\ ,$$

where τ and τ_x are surface wind stress and its east-west component, respectively, and β is the latitudinal variation of the Coriolis parameter. Upwelling favorable wind stress curl in the coastal ocean occurs when frictional retardation by land reduces equatorward wind stress on a western coast. *Fennel* [1999] showed theoretically that wind stress curl could have a substantial impact in coastal upwelling. Off Oregon, Ekman suction was a major contributor to the total upward velocity during coastal upwelling [*Halpern*, 1976].

[3] Off the west coast of South America, El Niño conditions include a deepening of the coastal thermocline [*Strub et al.*, 1998]. During the 1997–1998 El Niño in the coastal waters of southern Peru, the thermocline deepened by 75 m [*Grados*, 1998]. An enigma of El Niño off Peru is why the coastal thermocline deepens. *Wooster and Guillen* [1974] postulated that the deepened coastal thermocline off Peru during El Niño was a consequence of the *Bjerknes* [1969] breakthrough explanation about the weakening of the southeasterly tradewind as the fundamental generating mechanism of El Niño. Observations along the Pacific equator during the 1982–1983 El Niño confirmed the thermocline deepened when the southeasterly tradewind weakened [*Halpern*, 1987]. In contrast, at the coast of Peru during El Niño, $\tau_{alongshore}$ increased [*Enfield*, 1981; *Huyer et al.*, 1987], which would raise the thermocline. This paper will show with unprecedented fidelity that $\tau_{alongshore}$ increased over the coastal waters off Peru during the 1997–1998 El Niño. Throughout the seventy years of coastal upwelling studies off Peru, the effect of Ekman pumping/suction has received little attention because of the absence of suitable measurements. This paper shows how Ekman pumping may have deepened the thermocline during the 1997–1998 El Niño.

2. Data and Methods

[4] The most consistent and strongest upwelling center on the Peruvian coast occurs near San Juan at 15°S [*Longhurst*, 1998, p. 318]. Alongshore wind stress, which is representative of onshore-offshore Ekman transport, and Ekman pumping during the 1997–1998 El Niño are compared to those for May 1992 – April 1997 when oceanographic conditions were normal. The study interval began in May 1992 when final calibration of the scatterometer on the European Space Agency first European Remote-sensing Satellite (ERS-1) was completed. The ERS-1 scatterometer measured changes in radar backscatter at the sea surface to yield wind speed and direction referenced to 10-m height with an approximate 25-km × 25-km resolution. ERS-1 data (http://www.ifremer.fr/cersat) were continued with ERS-2, and the study interval arbitrarily concludes in December 1998. The root-mean-square error of 7-day averaged wind components was 0.8 m s^{-1} [*Quilfen et al.*, 2000].

[5] East-west and north-south wind stress components were computed from each ERS wind speed and direction with constant air density (1.225 kg m^{-3}) and a 10-m height drag coefficient dependent on wind speed [*Trenberth et al.*, 1990]. Wind stress components in 0.5° × 0.5° areas were averaged each calendar month. Monthly mean 0.5° × 0.5° values of W_{EK} and $\tau_{alongshore}$ were computed from monthly mean 0.5° × 0.5° wind stress components. Midpoints of the 0.5° × 0.5° $\tau_{alongshore}$ and W_{EK} values located closest to the coast were 27 km and 55 km, respectively.

[6] At 15°S the coast of Peru is aligned at an approximate 45° from north (Figure 1). Therefore, $\tau_{alongshore}$ was equal to the wind stress magnitude multiplied by $\cos\alpha$, where α is the difference of the directions of the wind stress and the 45° alignment of the coastline. From 14.5°S–15.0°S, the 0.5° × 0.5° area adjacent to the coast had sufficient ERS data, but from 15.0°S–15.5°S the 0.5° × 0.5° area adjacent to the coast did not have enough ERS data to merit inclusion in the analysis (Figure 1). Two 1°-latitude × 0.5°-longitude $\tau_{alongshore}$ values are described between 14.5°S and 15.5°S, with midpoints having offshore distances of 27 km and 135 km (Figure 1a). The W_{EK} centered at 15°S and 55 km from the

0094-8276/02/2001GL014097$05.00

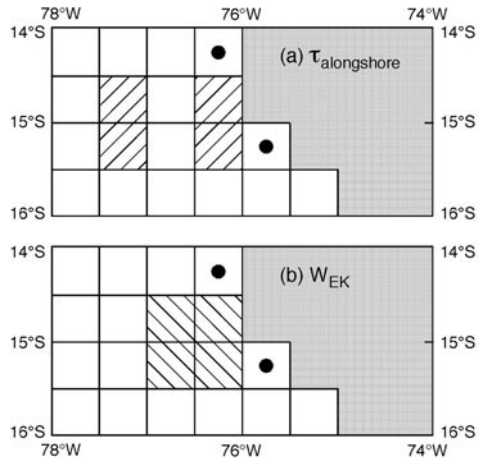

Figure 1. Locations of 0.5° × 0.5° areas used to compute $\tau_{alongshore}$ and W_{EK}. A region with a solid dot did not have sufficient data for analysis. Regions with hatch-lines in (a) were areas where $\tau_{alongshore}$ were analyzed and (b) comprised the area for the computation of W_{EK}. In (a), SST was analyzed in the near-shore region with hatch-lines. Gray region represents land.

coast was computed with four adjacent 0.5° × 0.5° wind stress Cartesian components in the 15.5°S–14.5°S, 77°W–76°W region (Figure 1b).

[7] Monthly mean 0.5° × 0.5° sea surface temperatures (SST) were computed from the Pathfinder data product (http://podaac.jpl.nasa.gov), with the same grid used for $\tau_{alongshore}$ (Figure 1a). The normal monthly mean SST was computed for the same interval as W_{EK} and $\tau_{alongshore}$.

[8] Assuming monthly mean values of a variable had a Gaussian distribution, a monthly anomaly is considered significant with 95% confidence if its absolute value is greater than twice the standard deviation during normal conditions. The 95% significance levels for $\tau_{alongshore}$, W_{EK} and SST were 2.6×10^{-2} N m^{-2}, 6.8×10^{-6} m s^{-1} and 1.2°C, respectively.

3. Results

[9] Coastal upwelling at 15°S was sustained throughout the year by offshore Ekman transport, which is represented by $\tau_{alongshore}$, and Ekman suction (Figure 2). At 27 km offshore, $\tau_{alongshore}$ had an annual cycle with maximum (7.4×10^{-2} N m^{-2}) in July–August and minimum (3.2×10^{-2} N m^{-2}) in January. The annual range (4.2×10^{-2} N m^{-2}) was substantially greater than the 95% significance level ($(=2.6/\sqrt{5} = 1.2) \times 10^{-2}$ N m^{-2}). At 55 km offshore, 5-year mean monthly fluctuations of W_{EK} were not 95% significantly different from one another. Annual mean $\tau_{alongshore}$ and W_{EK} were 5.1×10^{-2} N m^{-2} and 3.1×10^{-6} m s^{-1}, respectively.

[10] In June 1997, the $\tau_{alongshore}$ anomaly at 27 km from the coast was greater than the 95% significance level for the first time in three years and reached 4×10^{-2} N m^{-2} for the first time in 5 years (Figure 3a); the strengthening was two-thirds as large as the normal value for June (Figure 2a). The $\tau_{alongshore}$ anomaly remained above the 95% level in July and August, dipped slightly below in September, surged above the level in October, November, and December and then slowly returned to zero by April–May 1998. In July 1997, $\tau_{alongshore}$ was double its normal value (Figure 2a). The larger-than-normal $\tau_{alongshore}$ over coastal waters during the El Niño confirms a result from coastal data [*Enfield*, 1981; *Huyer et al.*, 1987]. During the 1997–1998 El Niño, $\tau_{alongshore}$ anomalies at 135 km offshore were similar to those at 27 km (Figure 3a), and from May–August 1997 the anomaly was larger closer to the coast.

[11] In May 1997, the W_{EK} anomaly was substantially downward (-7×10^{-6} m s^{-1}) (Figure 3b). It remained downward in June, July, and August 1997 with magnitudes greater, almost greater, and much greater, respectively, than the 95% significance level. In May–August 1997, the average W_{EK} anomaly (-9×10^{-6} m s^{-1}) was large enough to reverse the normal May–August upward W_{EK} (2.4×10^{-6} m s^{-1}). During the onset phase of the El Niño, W_{EK} was downward with a speed nearly four times greater than the normal upward speed. The anomalous downward motion occurred over a large area.

4. Discussion

[12] The following scenario explains how the upwelling favorable $\tau_{alongshore}$ increased during the 1997–1998 El Niño (Figure 3a). In normal conditions, SST was lower at the Peru coast compared to offshore, which is a characteristic of all coastal upwelling regimes. The resultant onshore-offshore atmospheric pressure difference would produce a geostrophic alongshore wind towards the south, i. e., in opposition to the prevailing tradewind. In May 1997, the SST anomaly at 27 km offshore had its largest magnitude (2.2°C) since the beginning of the study interval (Figure 3c). The May-to-July 1997 swiftness of the 6°C rise was stunning (Figure 3c), and in the coastal waters off Peru the 1997 winter SST was equivalent to summer SST (not shown). A consequence of intense ocean warming off Peru would be increased convection in the atmospheric planetary boundary layer, which reduced the prevalent occurrence of stratus clouds, warmed the air, and lowered barometric pressure [*Enfield*, 1981]. During austral winter of 1997, inland air temperature rose substantially above coastal air temperature [P. Lagos, personal communication, 1997], which would create a northward geostrophic wind to augment the southeast tradewind. In addition, during May–September 1997, the SST difference between 27 km and 135 km offshore was 50% smaller compared to normal conditions, which would reduce the strength of the poleward geostrophic wind component and, thereby, enhance the southeast tradewind.

[13] During the 1997–1998 El Niño the coastal thermocline off Peru deepened [*Grados*, 1998]; this feature has been observed during previous El Niños [*Strub et al.*, 1998]. Our analysis of Ekman pumping/suction at 15°S showed that Ekman pumping was very large during May–August 1997 of the El Niño. It is tempting to speculate that Ekman pumping could have caused the increase in the depth of the coastal thermocline. The downward displacement of the thermocline produced by the May–August 1997 W_{EK} (-9×10 m s^{-1}) would be about 90 m. This estimate is similar to the 75-m deepening in thermocline depth at 12°S, where measure-

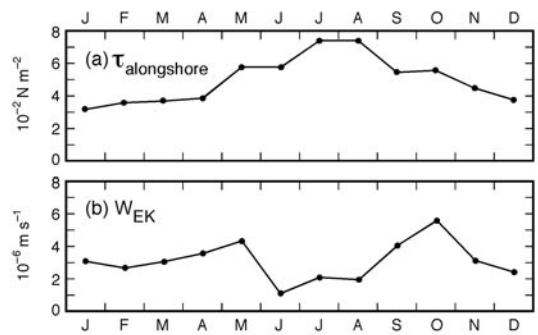

Figure 2. Mean monthly (a) alongshore wind stress ($\tau_{alongshore}$) at 14.5°S–15.5°S centered at 27 km offshore distance and (b) Ekman pumping/suction (W_{EK}) at 14.5°S–15.5°S centered at 55 km from the coast. Cross-shelf dimension of each region was 55 km in (a) and 110 km in (b).

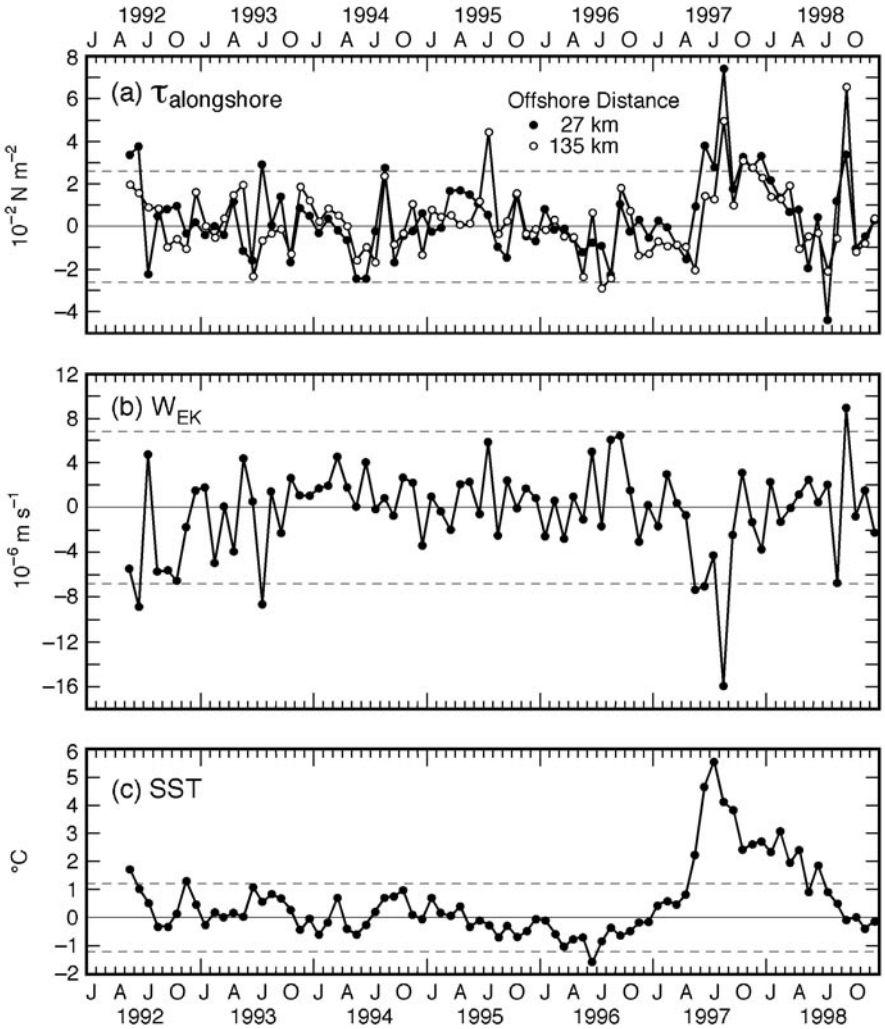

Figure 3. Monthly mean anomalies of (a) alongshore wind stress ($\tau_{alongshore}$), (b) Ekman pumping/suction (W_{EK}), and (c) sea surface temperature (SST). Locations are: (a) 14.5°S–15.5°S centered 27 km (solid circle) and 135 km offshore (open circle); (b) 14.5°S–15.5°S centered 55 km from the coast, and (c) 14.5°S–15.5°S centered 27 km offshore. Dash lines represent 95% confidence limits.

ments closest to 15°S were recorded during normal conditions and in January 1998 when El Niño observations were made [*Grados*, 1998]. In contrast, the increase in offshore Ekman transport beginning in June 1997 would tend to lift the thermocline if the thermocline had remained at its usual 25–50 m depth. Note that W_{EK} in May 1997 would have depressed the thermocline by 18 m. Convective mixing would not deepen the thermocline because El Niño water was warmer and less saline compared to the water below. An alternate mechanism to depress the thermocline would be geostrophic adjustment produced by a downwelling coastal Kelvin wave, which was observed at 20°30′S at the start of the 1997 El Niño [*Thomas et al.*, 2001].

5. Conclusion

[14] Satellite observations of ocean vector winds during 1992–1998 revealed two modes of coastal upwelling at 15°S. Both offshore Ekman transport and Ekman suction provided upward velocity during normal oceanographic conditions. However, each mode exhibited different behavior during the 1997–1998 El Niño when offshore Ekman transport increased compared to normal while normal mild Ekman suction was replaced with intense Ekman pumping. A weakness of our hypothesis of the substantial role of Ekman pumping to deepen the thermocline is the inability to discern a time delay between onsets of intense Ekman pumping and thermocline deepening and, also, to compare vertical displacements computed from W_{EK} with observations of thermocline deepening.

[15] **Acknowledgments.** Data processing was performed by Peter Woiceshyn, JPL, in his usual proficient manner. The work was supported by NASA RTOP 622-47-09. The research described in this paper was performed by the Jet Propulsion Laboratory, California Institute of Technology, under contract with the National Aeronautics and Space Administration.

References

Bjerknes, J., Atmospheric teleconnections from the equatorial Pacific, *Mon. Wea. Rev.*, *97*, 163–172, 1969.

Enfield, D. B., Thermally driven wind variability in the planetary boundary layer above Lima, Peru, *J. Geophys. Res.*, *86*, 2005–2016, 1981.

Fennel, W., Theory of the Benguela upwelling system, *J. Phys. Oceanogr.*, *29*, 177–190, 1999.

Grados, C., Informativo Oceanografico, No. 8, in http://www.imarpe. gob.pe, 1998.

Halpern, D., Measurements of near-surface wind stress over an upwelling region near the Oregon coast, *J. Phys. Oceanogr.*, *6*, 108–112, 1976.

Halpern, D., Observations of annual and El Niño thermal and flow variations along the equator at 0°, 110°W and 0°, 95°W during 1980–1985, *J. Geophys. Res.*, *92*, 8197–8212, 1987.

Huyer, A., R. L. Smith, and T. Paluszkiewicz, Coastal upwelling off Peru during normal and El Niño times, 1981–1984, *J. Geophys. Res.*, *92*, 14,297–14,307, 1987.

Longhurst, A., *Ecological Geography of the Sea*. Academic Press, 398 pp., 1998.

Quilfen, Y., A. Bentamy, P. Delecluse, K. Katsaros, and N. Grima, Prediction of sea level anomalies using ocean circulation model forced by scatterometer wind and validation using TOPEX/Poseidon data, *IEEE Trans. Geosci. Remote Sensing*, *38*, 1871–1884, 2000.

Stommel, H. M., *The Gulf Stream*: *A Physical and Dynamical Description*, 202 pp., Univ. Calif. Press, Berkeley, Calif., 1958.

Strub, P. T., J. Mesias, V. Montecino, J. Rutllant, and S. S. Marchant, Coastal ocean circulation off western South America, in *The Sea*, vol. 11, edited by A. R. Robinson and K. H. Brink, pp. 273–314, John Wiley, New York, 1998.

Sverdrup, H. U., M. W. Johnson, and R. H. Fleming, *The Oceans: Their Physics, Chemistry, and General Biology*, 1087 pp., Prentice-Hall, Englewood Cliffs, New Jersey, 1942.

Thomas, A. C., J. L. Blanco, M. E. Carr, P. T. Strub, and J. Osses, Satellite-measured chlorophyll and temperature variability off northern Chilew during the 1996–1998 La Niña and El Niño, *J. Geophys. Res.*, *106*, 899–915, 2001.

Trenberth, K. E., W. G. Large, and J. G. Olson, The mean annual cycle of the global ocean wind stress, *J. Phys. Oceanogr.*, *20*, 1742–1760, 1990.

Wooster, W. S., and O. Guillen, Characteristics of El Niño in 1972, *J. Mar. Res.*, *32*, 387–404, 1974.

D. Harpern, Jet Propulsion Laboratory, California Institute of Technology, Pasadena, CA 91109, USA.